

UNCLASSIFIED

AD 4 3 9 2 4 4

DEFENSE DOCUMENTATION CENTER

FOR

SCIENTIFIC AND TECHNICAL INFORMATION

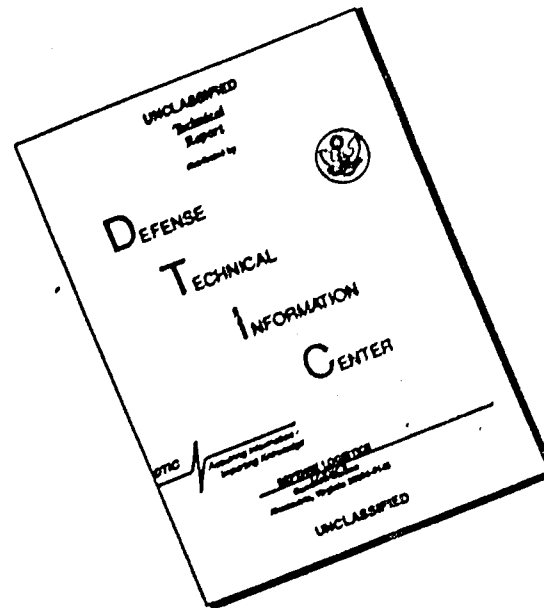
CAMERON STATION, ALEXANDRIA, VIRGINIA



UNCLASSIFIED

NOTICE: When government or other drawings, specifications or other data are used for any purpose other than in connection with a definitely related government procurement operation, the U. S. Government thereby incurs no responsibility, nor any obligation whatsoever; and the fact that the Government may have formulated, furnished, or in any way supplied the said drawings, specifications, or other data is not to be regarded by implication or otherwise as in any manner licensing the holder or any other person or corporation, or conveying any rights or permission to manufacture, use or sell any patented invention that may in any way be related thereto.

DISCLAIMER NOTICE



THIS DOCUMENT IS BEST QUALITY AVAILABLE. THE COPY FURNISHED TO DTIC CONTAINED A SIGNIFICANT NUMBER OF PAGES WHICH DO NOT REPRODUCE LEGIBLY.

64-13

SSD-TDR-64-29

CATALOGED BY DDC

AS AD NO. 439244

439244

Simulation of a Thin Plasma Sheath by a Plane of Wires

30 MARCH 1964

*Prepared by K. E. GOLDEN and T. M. SMITH
Plasma Research Laboratory*

Prepared for COMMANDER SPACE SYSTEMS DIVISION

UNITED STATES AIR FORCE

Inglewood, California

MAY 15 1964



LABORATORY OPERATIONS • AEROSPAC CORPORATION
CONTRACT NO. AF 04(695)-269

SIMULATION OF A THIN PLASMA SHEATH
BY A PLANE OF WIRES

Prepared by
K. E. Golden and T. M. Smith
Plasma Research Laboratory

AEROSPACE CORPORATION
El Segundo, California

Contract No. AF 04(695)-269

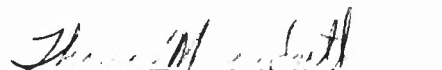
30 March 1964

Prepared for
COMMANDER SPACE SYSTEMS DIVISION
UNITED STATES AIR FORCE
Inglewood, California

SIMULATION OF A THIN PLASMA SHEATH
BY A PLANE OF WIRES

Prepared by:


K. E. Golden


T. M. Smith

Approved by:


R. H. Huddleston, Head
Plasma Physics Department


R. X. Meyer, Director
Plasma Research Laboratory

This technical documentary report has been reviewed and is approved for publication and dissemination. The conclusions and findings contained herein do not necessarily represent an official Air Force position.

For Space Systems Division
Air Force Systems Command:


Kenneth R. Hughey
Captain, USAF

AEROSPACE CORPORATION
El Segundo, California

ABSTRACT

A method of simulating a thin plasma sheath of the type encountered in some aerospace applications by using a single plane of equally spaced wires is described. It is shown that the surface impedance of such a periodic structure can be made equal to that of a thin plasma sheath. In this treatment, the respective surface impedances are related through three dimensionless parameters. A simple technique for obtaining high losses is also discussed, whereby collision frequencies in the neighborhood of the operating frequency are realizable.

Experimental data, including both the lossy and lossless cases, are compared with the theoretical model in the X-band region.

CONTENTS

I.	INTRODUCTION	1
II.	PLASMA SURFACE IMPEDANCE	1
III.	WIRE GRID STRUCTURE	5
IV.	EQUIVALENCE BETWEEN PLASMA AND PERIODIC STRUCTURE	7
V.	PRACTICAL CONSIDERATIONS	8
VI.	REFLECTION AND TRANSMISSION COEFFICIENTS	9
VII.	EXPERIMENTAL DATA	12
VIII.	SUMMARY	28
	REFERENCES	29

FIGURES

1a.	Equivalent Sheath Problem for Jump Conditions	3
1b.	Slab Problem	3
2.	Equivalent Wire Grid Structure	6
3a.	Lossy Wire Grid Structure.	10
3b.	Wire Screen Structure	10
4.	Grid Structure in X-band Waveguide	13
5.	Diagram of the X-band Waveguide Interferometer	15
6.	X-band Waveguide Test Section	17
7.	Lossless Reflection Magnitude Data	18
8.	Lossless Reflection Phase Data	19
9.	Reflection and Transmission Data for an Equivalent Collision Frequency of 1.476 Gc	20
10.	Transmission Phase Data for an Equivalent Collision Frequency of 1.476 Gc	21
11.	Reflection and Transmission Data for an Equivalent Collision Frequency of 4.95 Gc	22
12.	Transmission Phase Data for an Equivalent Collision Frequency of 4.95 Gc	23
13.	Reflection and Transmission Data for an Equivalent Collision Frequency of 12.82 Gc	24
14.	Transmission Phase Data for an Equivalent Collision Frequency of 12.82 Gc	25
15.	Reflection and Transmission Data for an Equivalent Collision Frequency of 126 Gc	26
16.	Transmission Phase Data for an Equivalent Collision Frequency of 126 Gc	27

I. INTRODUCTION

The simulation of the electromagnetic properties of a plasma sheath, such as those encountered with a slender body re-entry vehicle, would be useful in laboratory antenna pattern measurements. The main objective of this report is to develop a technique of simulating the reflection and transmission characteristics of a very thin sheath. The sheath will be assumed to be overdense or to be operating below the plasma frequency. The thickness of the sheath is assumed to be very small compared with a wavelength, thus making radio transmission possible.

In 1962 it was observed (Ref. 1) that the complex dielectric constant of a plasma slab could be simulated by a rodged medium. Physically, the currents induced in the rods behave like the oscillatory currents in a plasma making the simulation possible. In many cases, however, simulating a thin overdense plasma with an artificial dielectric is difficult because of fabrication limitations. For example, the simulation of a sheath with a thickness equal to $1/50 \lambda_o$ requires the spacing between adjacent rods to be equal to or less than a $1/50 \lambda_o$.

It will be shown that a wire grating structure behaves like a thin overdense plasma by simulating the equivalent surface current density of the sheath. It is obvious that the wires cannot simulate all the complexities of an actual re-entry plasma, but at this stage the simulation of the simplest properties can prove to be very useful in antenna evaluation and design.

II. PLASMA SURFACE IMPEDANCE

The first step in the development is to understand that which characterizes the reflection and transmission properties of the sheath. For the purpose of this analysis, the sheath is assumed to be an infinite slab with a uniform plane

wave reflecting off its surface at an angle Θ , as shown in Fig. 1a. When the sheath is overdense and very thin, it looks like an inductive surface current to the incident electromagnetic signal. Therefore, it should be possible to simulate the sheath's characteristics by replacing it with an equivalent surface current density. It is interesting to note that J. Wait (Ref. 2) and other authors have used this technique to obtain approximate solutions to complex boundary value problems.

The jump condition used by Wait can be developed by applying Ampere's Law and Faraday's Law to a rectangular circuit as shown in Fig. 1b. The application of Faraday's Law leads to the continuity of the tangential E field across the sheath. The surface current, which is equal to the discontinuity of the tangential H field, is obtained by using Ampere's Law.

$$\Delta E_t = 0 \quad (1)$$

$$\Delta H_t = J_s \quad (2)$$

The surface current J_s is determined by

$$J_s = \sigma d E_1 \quad (3)$$

where σ is the complex conductivity of the sheath, d is the sheath thickness, and E_1 is the tangential electric field at the surface. The reflection and transmission properties of the sheath are, therefore, governed solely by the equivalent surface current density J_s . The surface impedance Z_{sp} is related to Eq. (3) through Ohm's Law

$$Z_{sp} = \frac{E_1}{J_s} \text{ (ohms/square)}$$

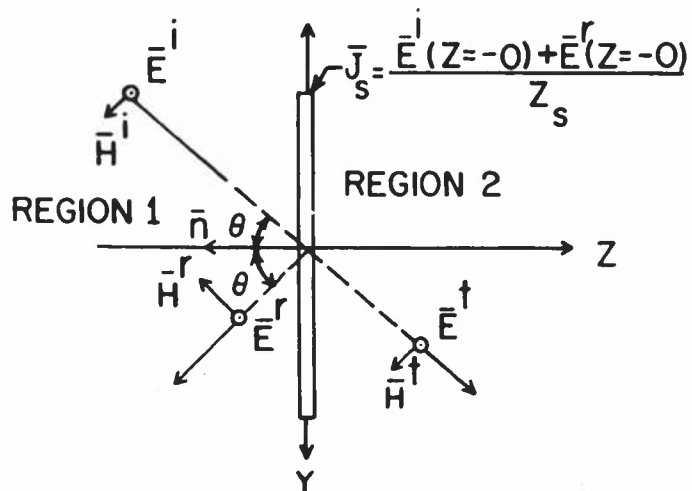


Fig. 1a. Equivalent Sheath Problem for Jump Conditions

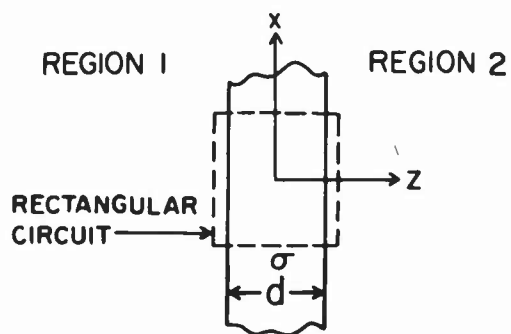


Fig. 1b. Slab Problem

The resulting surface impedance for a thin plasma is

$$Z_{sp} = \frac{1}{\sigma d} \quad (4)$$

The well-known expression for conductivity of a cold plasma (Ref. 3) is

$$\sigma = \frac{\epsilon_o \omega_p^2}{\nu_c + j\omega}$$

where ν_c is the collision frequency and ω_p is the plasma frequency. The surface impedance reduces to

$$Z_{sp} = \frac{\nu_c + j\omega}{\epsilon_o \omega_p^2 d}$$

when σ is substituted into Eq. (4). The last equation can be expressed in terms of three nondimensional quantities, W , V and D .

$$Z_{sp} = Z_o \left(\frac{V}{W^2 D} + j \frac{1}{W^2 D} \right) \quad (5)$$

$$W = \frac{\omega_p}{\omega} \quad (6)$$

$$V = \frac{\nu_c}{\omega} \quad (7)$$

$$D = k_o d \quad (8)$$

$$Z_o = \sqrt{\frac{\mu_o}{\epsilon_o}} = 377 \text{ ohms/square}$$

The free space propagation constant, k_o , is defined as follows

$$k_o = \frac{\omega}{c} = \frac{2\pi}{\lambda_o}$$

The surface impedance of the sheath is equivalent to a series RL circuit. The resistive term is associated with the loss mechanism in the plasma, and the reactive part is related to the phase difference between the motion of the electrons and the applied electric field.

The basic assumptions associated with the jump conditions (Ref. 4) are (1) the frequency, ω , and the thickness, d , must be such that the flux linking the rectangular circuit is negligible, and (2) the fields inside the plasma have only z dependence. These assumptions are satisfied when

$$\frac{\omega_p}{\omega} \gg 1$$

and

$$k_o d \ll 1$$

III. WIRE GRID STRUCTURE

The behavior of a plane of equally spaced wires has been discussed at some length by various authors (Refs. 5, 6 and 7). In the case under consideration, the electric field is assumed to be parallel to the wires as shown in Fig. 2. When the diameter of the wires is much less than the wire spacing and the

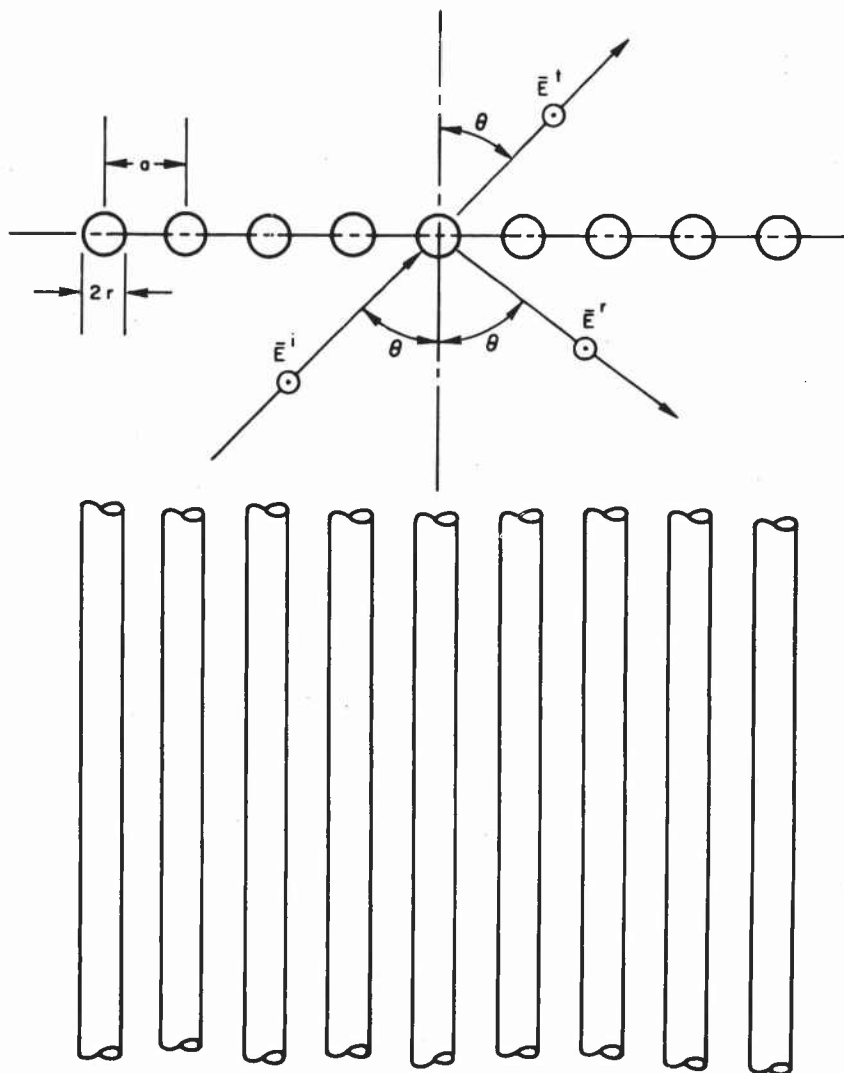


Fig. 2. Equivalent Wire Grid Structure

spacing is less than a half a wavelength, then the surface impedance of the grid structure (Refs. 8 and 9) can be shown to equal

$$Z_{sw} = R_s + jZ_o \frac{a}{\lambda_o} \ln\left(\frac{a}{2\pi r}\right) \quad (9)$$

where a is the spacing between adjacent wires, r is the radius of the wires, and λ_o is the free space wavelength. If the wire spacing becomes greater than half a wavelength, the grid structure starts to take on the character of an optical grating and the appearance of more than one reflected beam is sometimes observed. The internal surface resistance, R_s , of a grid structure, consisting of n wires per unit width, is equivalent to the resistance per unit length of n wires in parallel. It follows that

$$R_s = aR_o \quad (10)$$

where R_o is the internal resistance per unit length of one wire.

IV. EQUIVALENCE BETWEEN PLASMA AND PERIODIC STRUCTURE

Next in the development is the comparison of the surface impedance of the wires with that of the plasma sheath. The surface impedance of the plasma sheath is given by Eq. (5) and the wire grid structure by Eq. (9).

$$Z_{sp} = \frac{Z_o V}{W_D^2} + j \frac{Z_o}{W_D^2}$$

$$Z_{sw} = R_s + jZ_o \frac{a}{\lambda_o} \ln\left(\frac{a}{2\pi r}\right)$$

If one notes that both impedances have a resistance and an inductive reactance, then the relations connecting the wire grid and plasma sheath parameters are found by equating the real and imaginary parts of the respective impedances.

$$\frac{R_s}{Z_o} = \frac{V}{W^2 D} \quad (11)$$

$$\frac{a}{\lambda_o} \ln\left(\frac{a}{2\pi r}\right) = \frac{1}{W^2 D} \quad (12)$$

Equations (11) and (12) are then reduced to the following:

$$\frac{R_s}{Z_o} = \frac{c v_c}{\omega_p^2 d}$$

$$\frac{a \ln\left(\frac{a}{2\pi r}\right)}{\lambda_o} = \frac{2\pi c^2}{\lambda_o \omega_p^2 d}$$

$$c = \frac{1}{\sqrt{\mu_o \epsilon_o}}$$

indicating that the simulation is independent of frequency. Equations (11) and (12) constitute the equations used to design a wire grid structure having an equivalent W , D , and V .

V. PRACTICAL CONSIDERATIONS

High collision frequencies require large surface resistance as seen from Eq. (11). The surface resistance, R_s , must be of the order of 500 ohms per

square, if collision frequencies in the neighborhood of the operating frequency are desired. One promising method of obtaining large internal resistance consists of coating quartz fibers with a thin metallic layer of thickness t , (see Fig. 3a). By making the thickness of the metallic layer much less than a skin depth, the resulting internal resistance is independent of frequency and is given by

$$R_o = \frac{1}{\sigma_m 2\pi r t} \text{ (ohms/meter)} \quad (13)$$

where σ_m is the conductivity of the metallic layer. With this technique, resistances of 1000 ohms per inch have been obtained.

The equally spaced wires will only simulate the inductive character of the plasma when the electric field is parallel to the wires. When the electric field is perpendicular to the wires, the incident wave is practically unaltered by their presence. A more detailed analysis (Ref. 10) shows that the surface admittance is small for this polarization. A thin plasma sheath can be simulated by a square lattice screen structure independent of the polarization (see Fig. 3b). The incident electric field can be separated into two components, each one parallel to one set of wires. The resulting surface impedance is given by Eq. (9).

VI. REFLECTION AND TRANSMISSION COEFFICIENTS

The reflection and transmission coefficients for the plane of wires and the plasma sheath can be derived from the jump conditions given in Eqs. (1) and (2). Assume that a plane wave is incident at an angle θ from the left and the electric field is parallel to the plane of the interface as shown in Fig. 2.

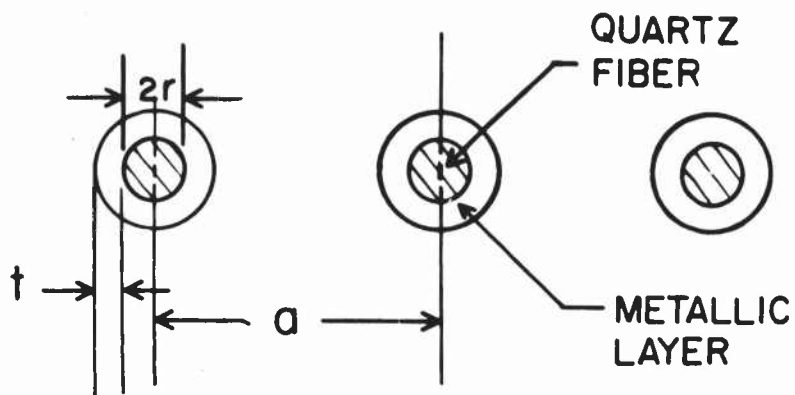


Fig. 3a. Lossy Wire Grid Structure

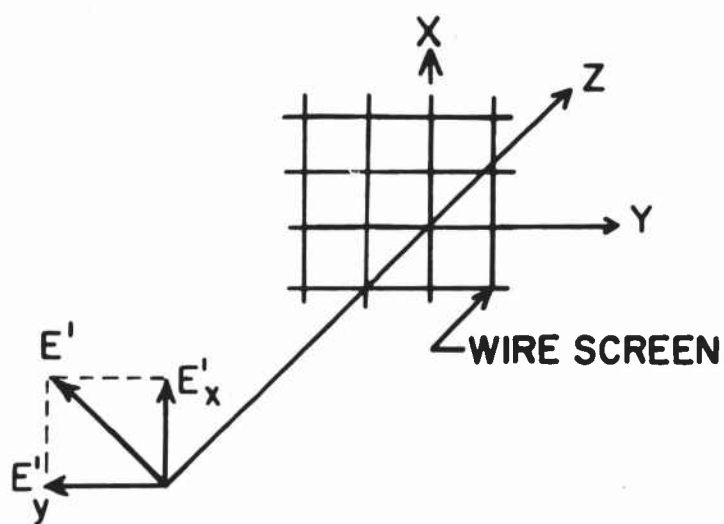


Fig. 3b. Wire Screen Structure

Application of the jump conditions, Eqs. (1) and (2), to this geometry yields

$$(H^i + H^r - H^t) \cos \theta = \frac{E^i + E^r}{Z_s} \quad (14)$$

$$(E^i + E^r - E^t) = 0 \quad (15)$$

Since the incident, reflected, and transmitted fields are uniform plane waves, the electric field is related to magnetic field through an intrinsic impedance Z_o . Use of this concept reduces Eq. (14) to

$$(E^i - E^r - E^t) \frac{\cos \theta}{Z_o} = \frac{E^i + E^r}{Z_s} \quad (16)$$

Solution of Eqs. (15) and (16) for the ratio E^r/E^i leads to a reflection coefficient given by

$$r = \frac{-1}{2Z_s \cos \theta + \frac{Z_o}{1}} \quad (17)$$

In a similar manner, the transmission coefficient is obtained by solving Eqs. (15) and (16) for the ratio E^t/E^i

$$t = \frac{1}{Z_o + \frac{2Z_s \cos \theta}{1}} \quad (18)$$

The reflection and transmission coefficients for the thin plasma sheath are obtained by substituting the surface impedance given by Eq. (5) into Eqs. (17) and (18).

$$R_p = \frac{-1}{1 + \frac{2V \cos \Theta}{W^2_D} + j \frac{2 \cos \Theta}{W^2_D}} \quad (19)$$

$$T_p = \frac{\frac{2V \cos \Theta}{W^2_D} + j \frac{2 \cos \Theta}{W^2_D}}{1 + \frac{2V \cos \Theta}{W^2_D} + j \frac{2 \cos \Theta}{W^2_D}} \quad (20)$$

Similarly, the reflection and transmission coefficients for the wire grid structure are given by

$$R_w = \frac{-1}{1 + \frac{2R_s}{Z_o} \cos \Theta + j \frac{2a}{\lambda_o} \cos \Theta \ln\left(\frac{a}{2\pi r}\right)} \quad (21)$$

$$T_w = \frac{\frac{2R_s}{Z_o} \cos \Theta + j \frac{a}{\lambda_o} \cos \Theta \ln\left(\frac{a}{2\pi r}\right)}{1 + \frac{2R_s}{Z_o} \cos \Theta + j \frac{2a}{\lambda_o} \cos \Theta \ln\left(\frac{a}{2\pi r}\right)} \quad (22)$$

The subscripts p and w denote the quantities pertaining to the thin plasma sheath and the wire grid structure, respectively.

VII. EXPERIMENTAL DATA

The reflection and transmission properties of different wire grid structures were measured in an X-band waveguide geometry. The dominant TE_{10} mode in a rectangular waveguide is analogous to two uniform plane waves bouncing off the walls of the waveguide as shown in Fig. 4 (Ref. 11). The equivalent

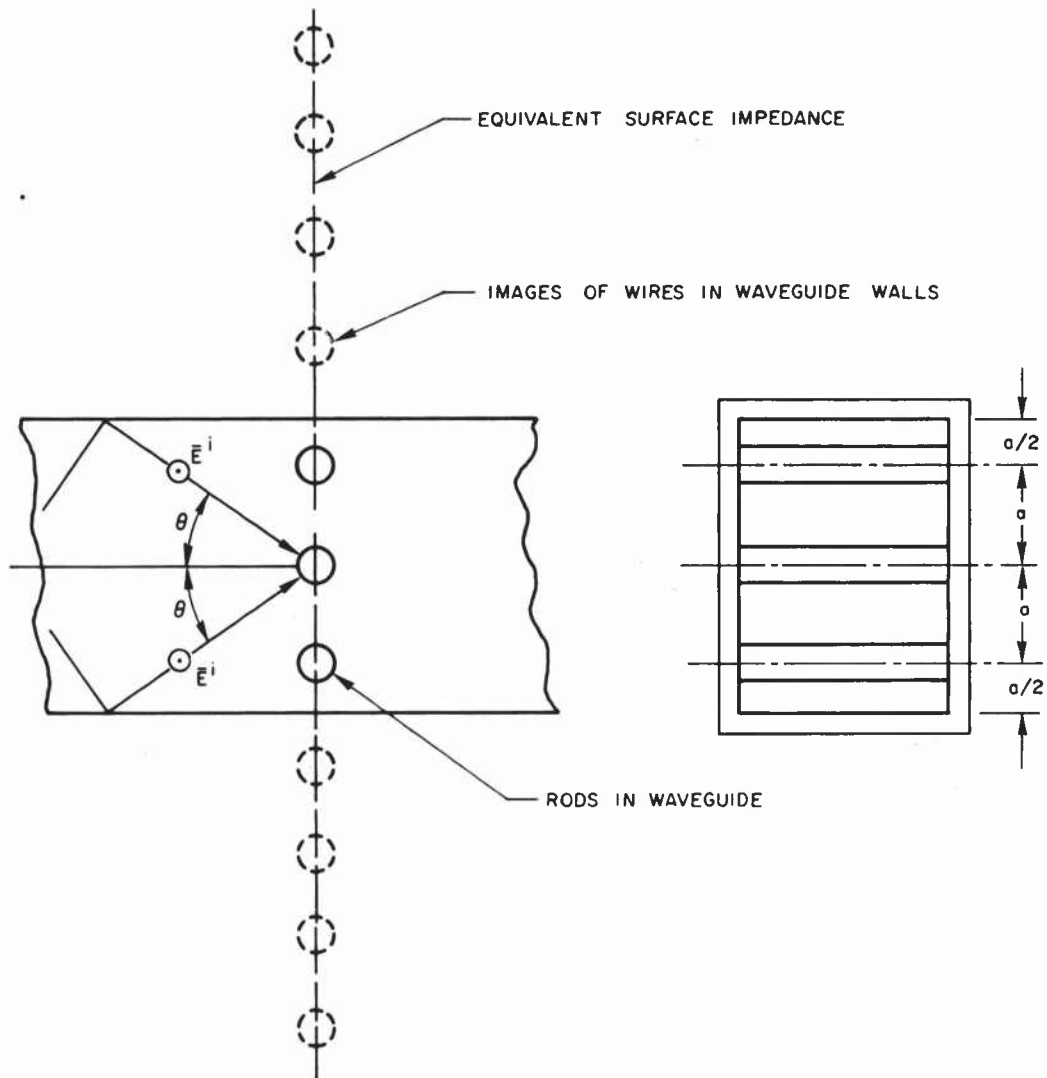


Fig. 4. Grid Structure in X-band Waveguide

angle of incidence, θ , of these two waves is related to the waveguide impedance and waveguide wavelength as shown below:

$$Z_g = \frac{Z_o}{\cos \theta} \quad (23)$$

$$\lambda_g = \frac{\lambda_o}{\cos \theta} \quad (24)$$

With this in mind, the measurements obtained in the waveguide geometry are equivalent to the same measurements performed in free space but at an angle of incidence given by Eqs. (23) and (24). The equations governing the complex reflection and transmission coefficients for the wire structure in the waveguide geometry are obtained by substituting Eqs. (23) and (24) into Eqs. (21) and (22).

$$R_w = \frac{-1}{1 + 2(R_s/Z_g) + j \left[2a \ln\left(\frac{a}{2\pi r}\right) / (\lambda_g) \right]} \quad (25)$$

$$T_w = \frac{2(R_s/Z_g) + j \left[2a \ln\left(\frac{a}{2\pi r}\right) / (\lambda_g) \right]}{1 + 2(R_s/Z_g) + j \left[2a \ln\left(\frac{a}{2\pi r}\right) / (\lambda_g) \right]} \quad (26)$$

The experimental data were measured with an X-band waveguide interferometer shown in Fig. 5. The readings on the precision attenuator and phase shifter are related to the complex transmission coefficient of the sample being tested.

The slotted line located directly in front of the test section yields information pertaining to the reflection coefficient. The position of the nulls of the standing wave pattern are related to the reflection phase, and the VSWR reading

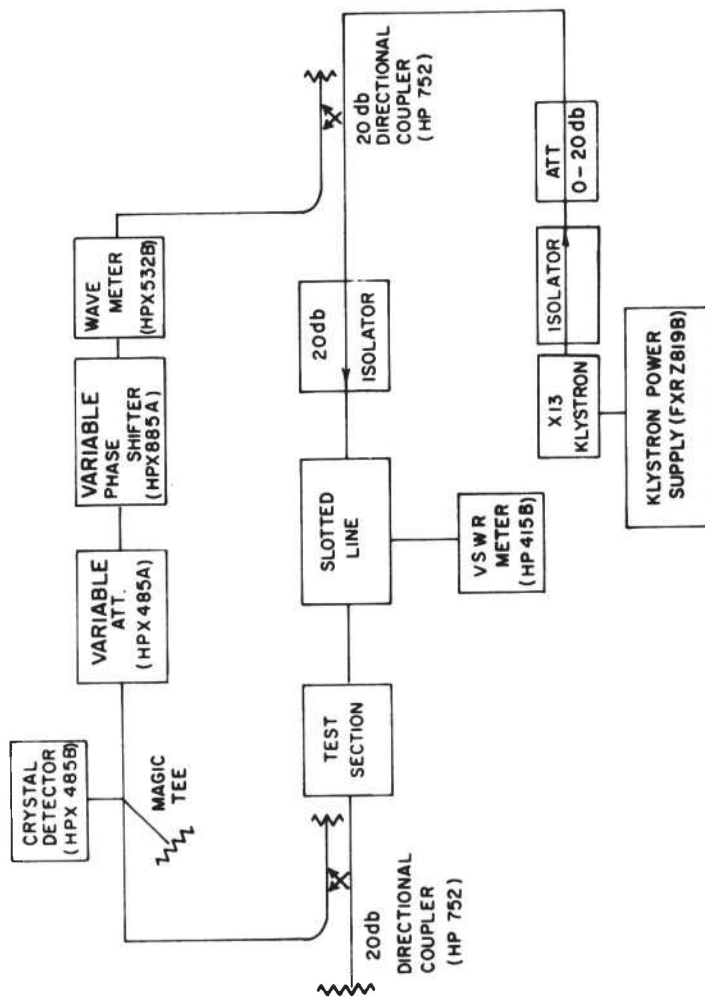


Fig. 5. Diagram of the X-band Waveguide Interferometer

yields the magnitude of the reflection coefficient. When the phase shift measurements are being performed, the probe antenna should be extracted from the slotted line.

The actual experiment consisted of measuring both the complex reflection and transmission coefficients for wire grid structures having a , ranging from 0.15 in. to 0.3 in. and r , ranging from 0.75 to 4.0 mils. The waveguide test section which holds the wire grid structure in place is shown in Fig. 6. The lossless data ($R_s = 0$) are plotted as a function of

$$\frac{\lambda_g}{a \ln\left(\frac{a}{2\pi r}\right)} = \frac{W^2 D}{\cos \Theta}$$

and compared with Eq. (25). The equivalent plasma frequency and thickness of the simulated sheath can be obtained from Eq. (12). Figures 7 and 8 summarize the measurements performed on the lossless copper wire models. As the diameter of the wire increases or the spacing decreases, the reflections off the grid structure become more severe as is seen in Fig. 7. The simulation of more dense plasma layers can therefore be accomplished either by using larger wires or by increasing the number of wires in the grid structure.

The experimental data for the lossy coated fibers are compared with Eqs. (25) and (26) in Figs. 9 through 16. The lossy wires are quartz fibers ranging from 1.5 to 4.0 mils in diameter with a gold pottery glaze fired on their surface. The value of R_s is obtained by measuring the linear resistance, R_o , with a dc ohmmeter and relating R_o to R_s by means of Eq. (10). The addition of losses in the grid structure tends to decrease the severity of the reflections, thereby increasing the transmission of electromagnetic energy as shown by the experimental data. The decrease in the reflection coefficient is attributed to the improved matching between the simulated sheath and its

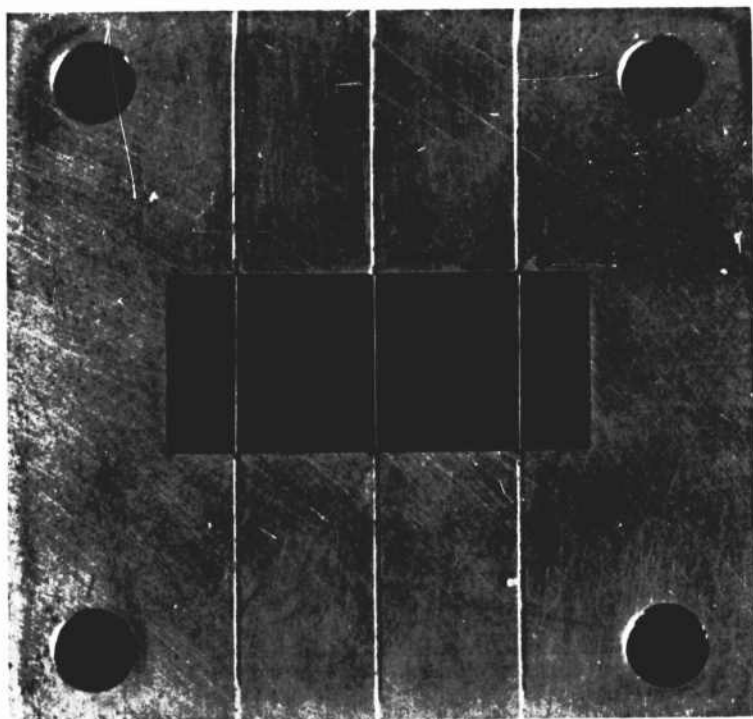


Fig. 6. X-band Waveguide Test Section

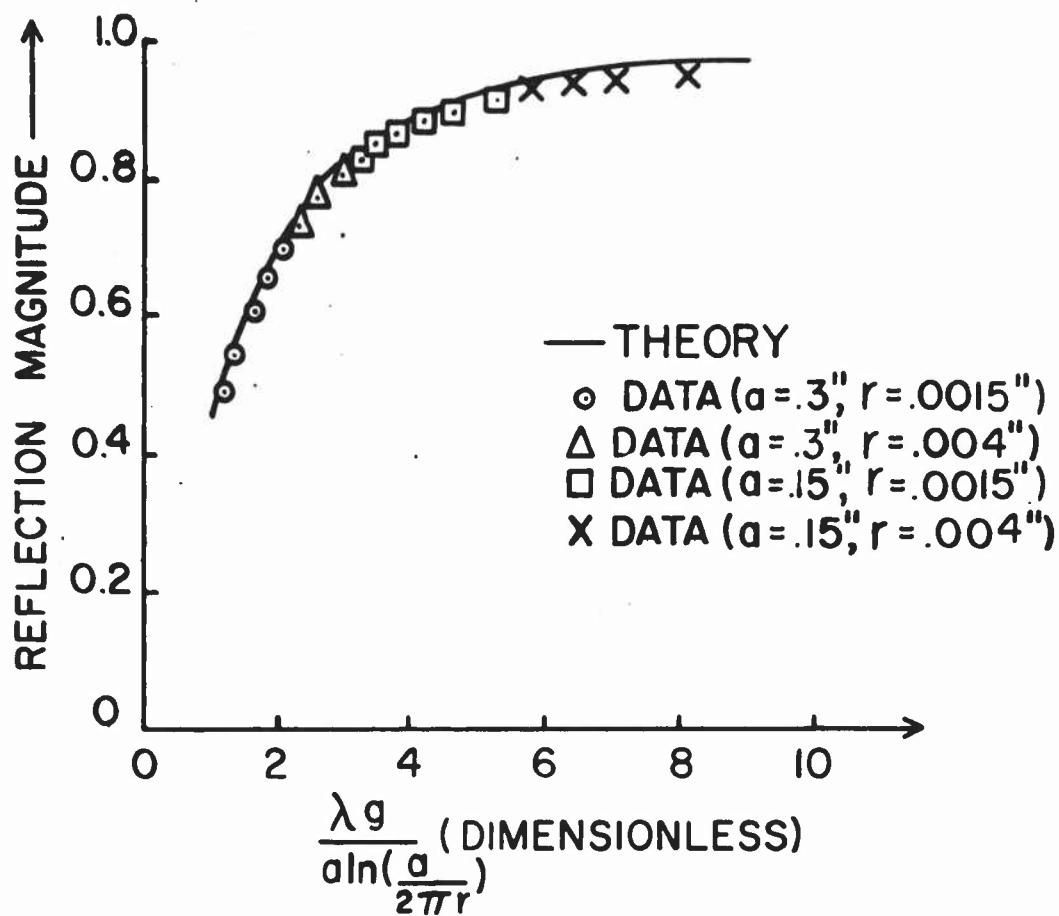


Fig. 7. Lossless Reflection Magnitude Data

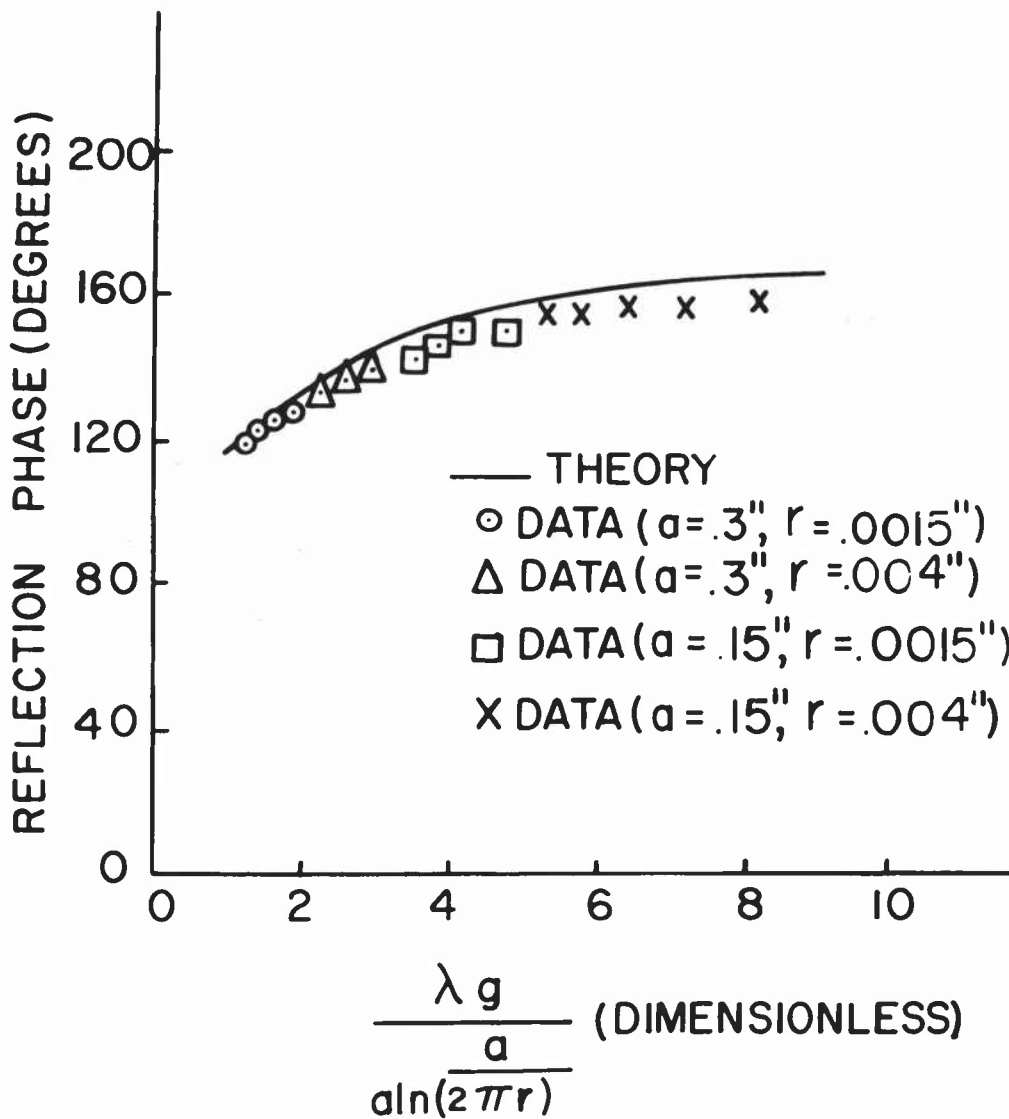


Fig. 8. Lossless Reflection Phase Data

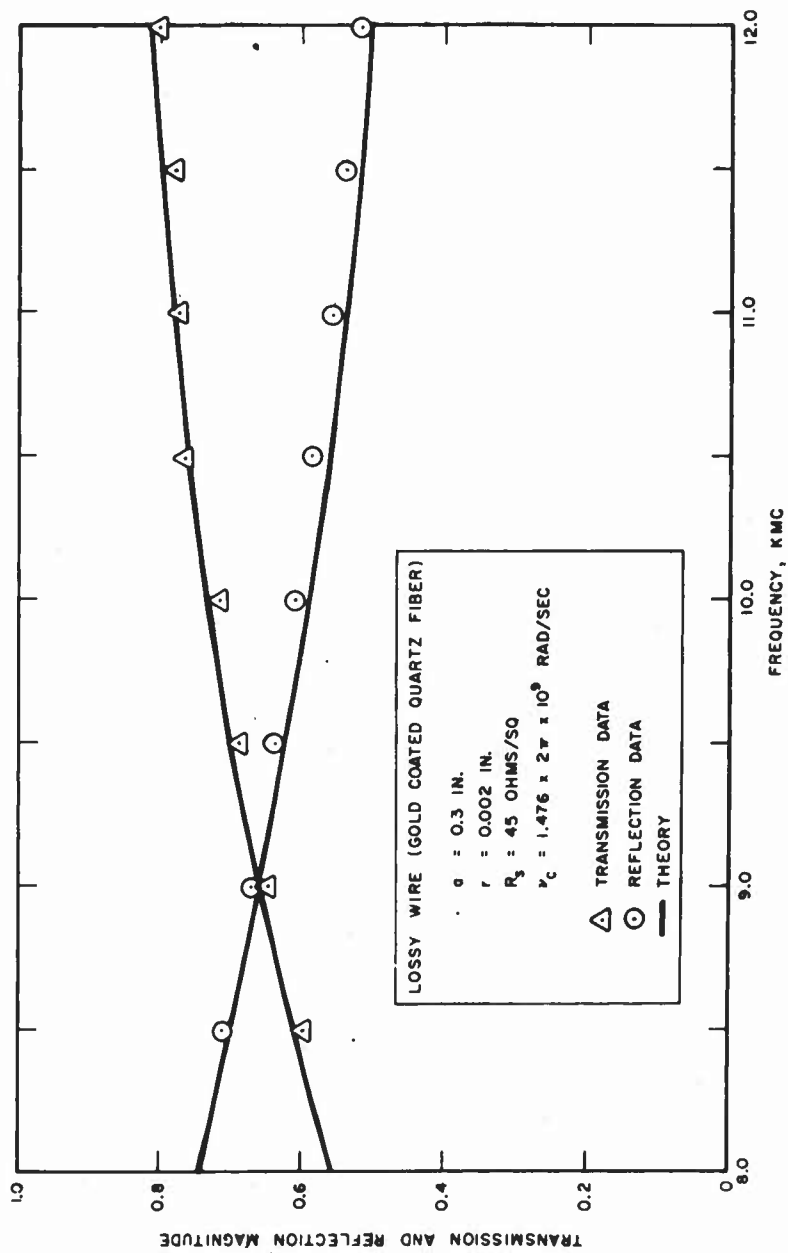


Fig. 9. Reflection and Transmission Data for an Equivalent Collision Frequency of 1.476 Gc

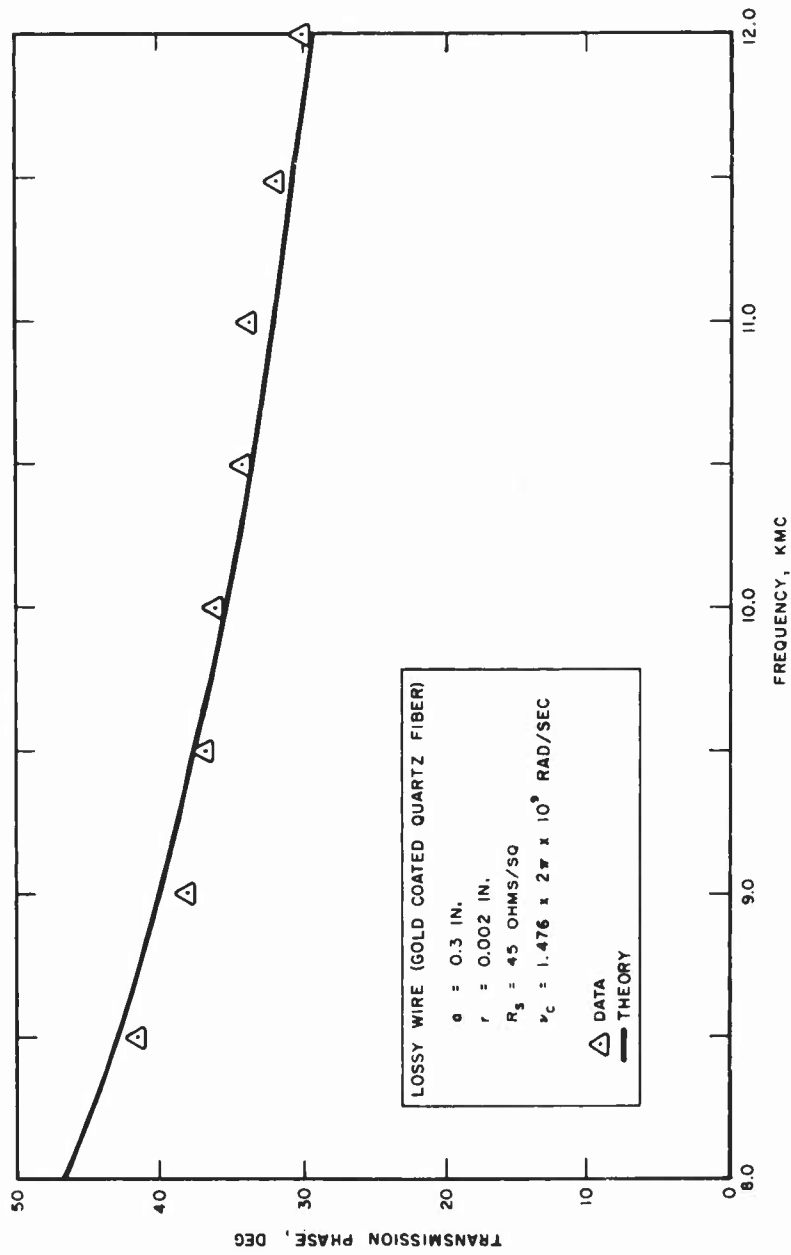


Fig. 10. Transmission Phase Data for an Equivalent Collision Frequency of 1.476 Gc

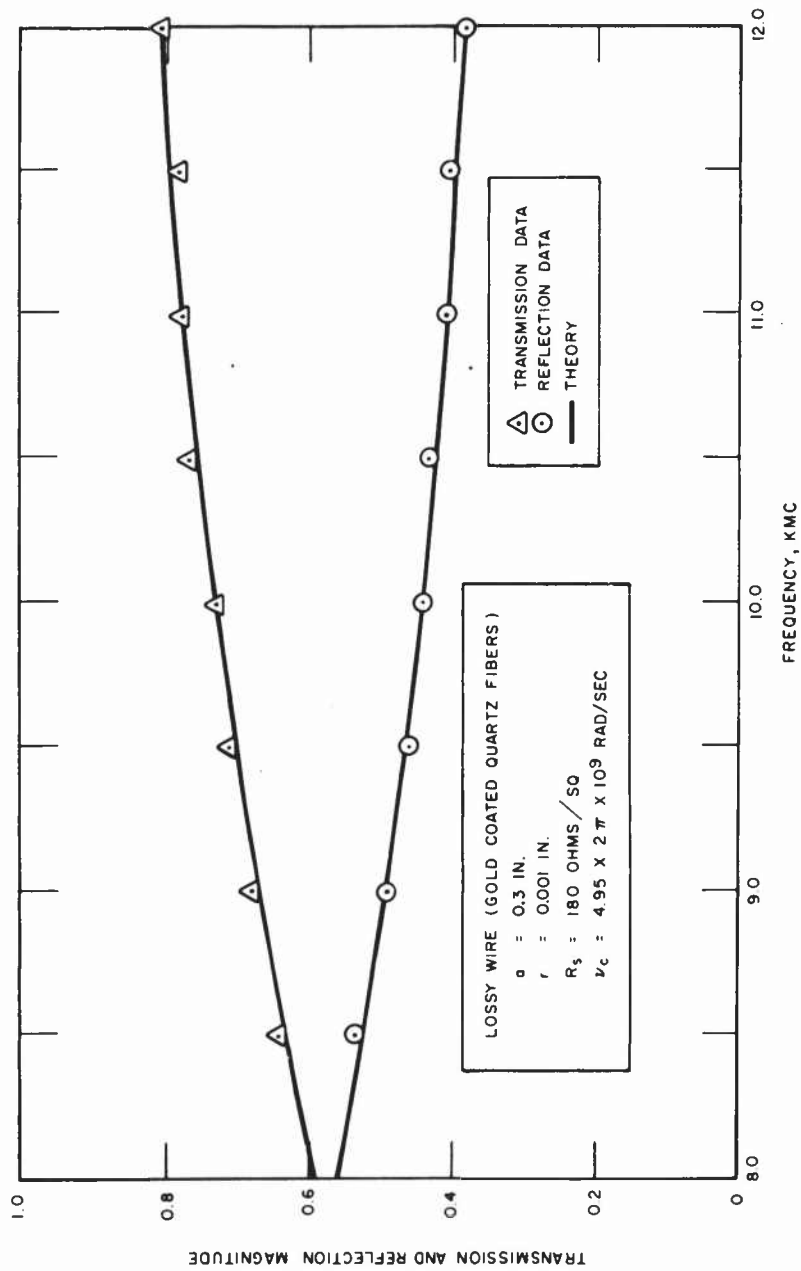


Fig. 11. Reflection and Transmission Data for an Equivalent Collision Frequency of 4.95 Gc

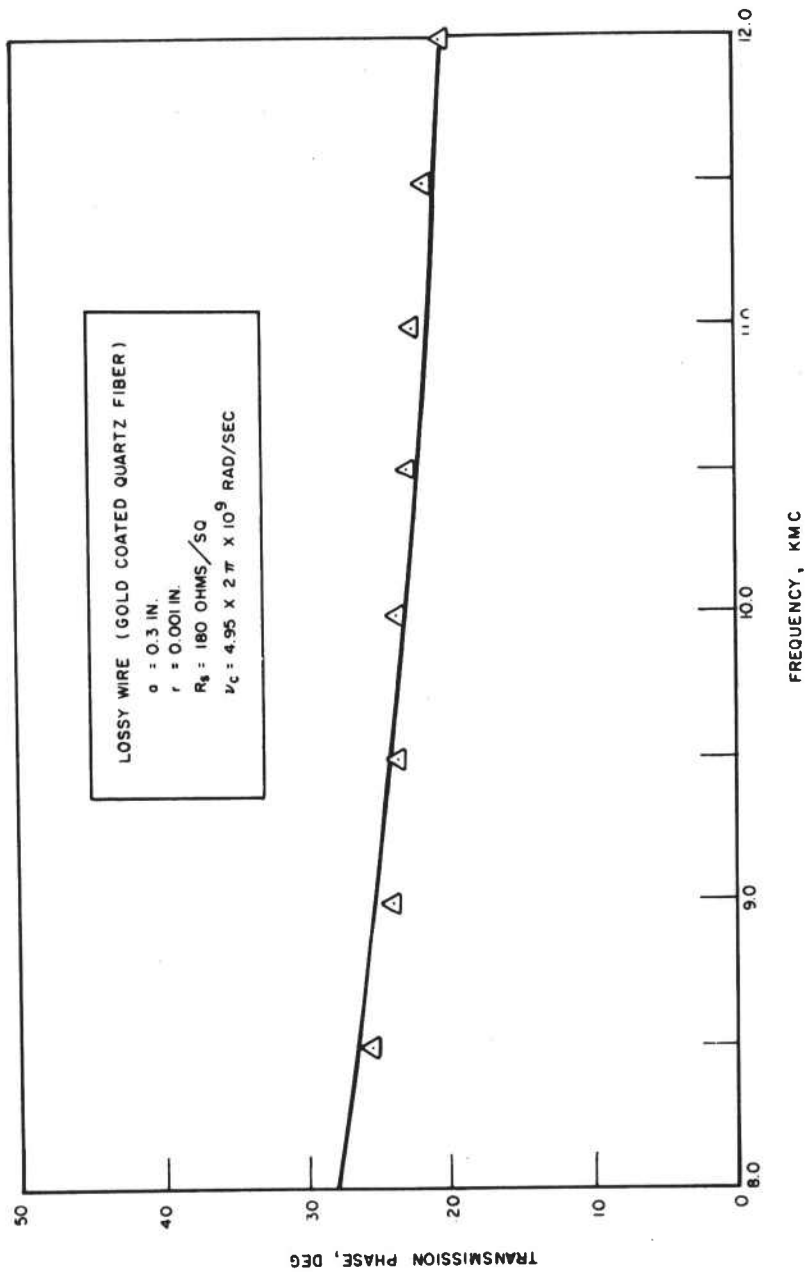


Fig. 12. Transmission Phase Data for an Equivalent Collision Frequency of 4.95 Gc

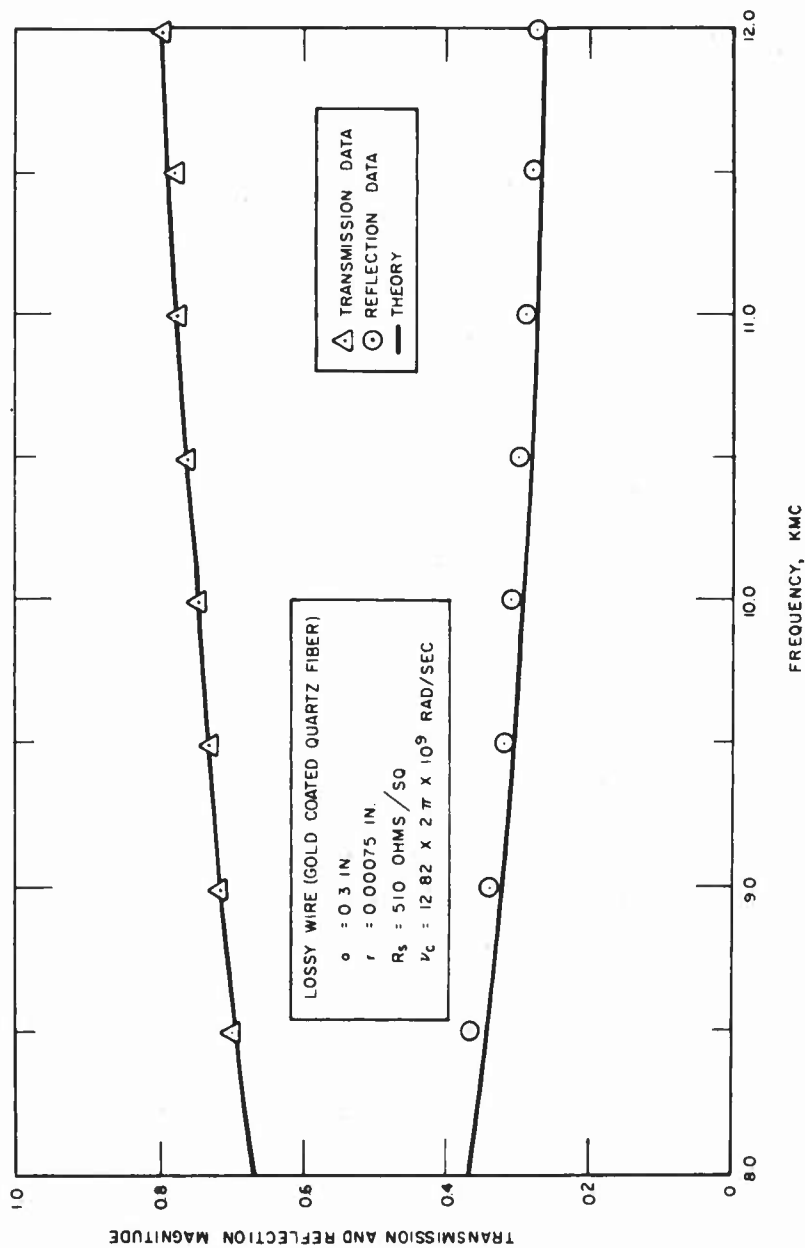


Fig. 13. Reflection and Transmission Data for an Equivalent Collision Frequency of 12.82 Gc

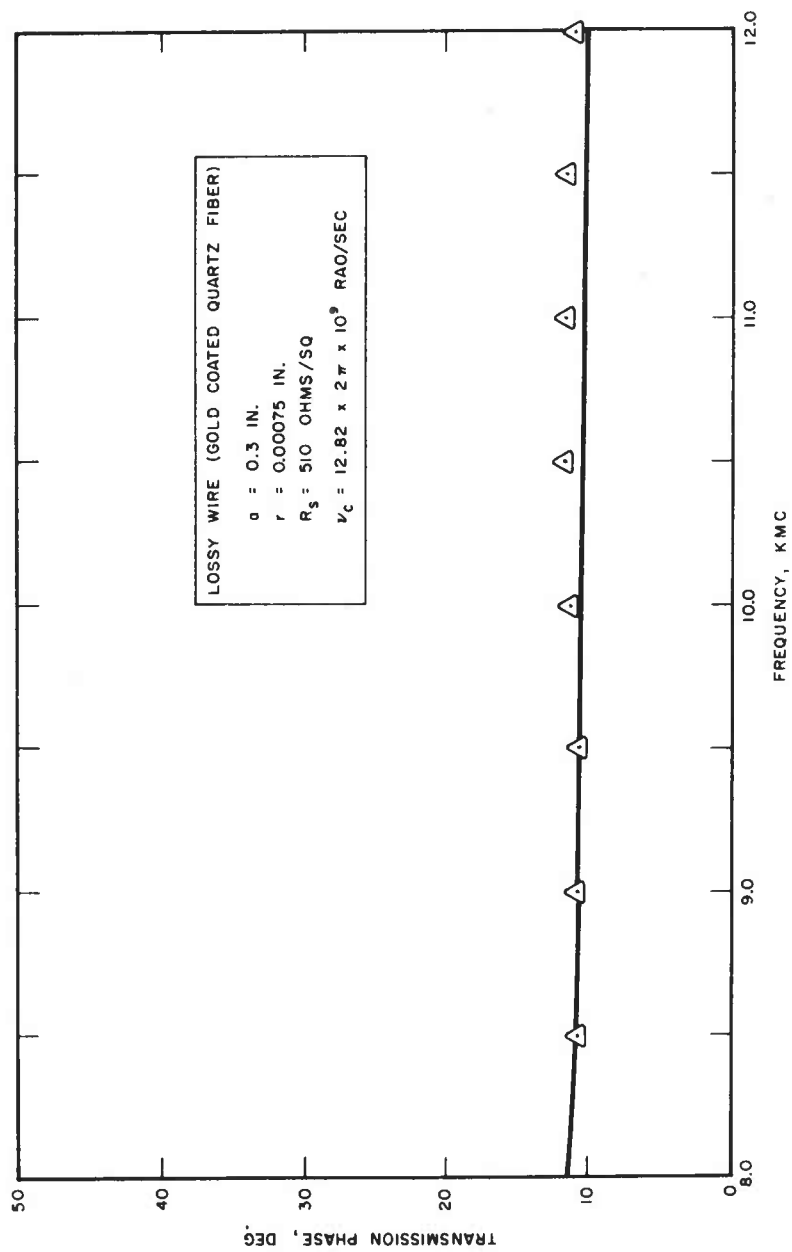


Fig. 14. Transmission Phase Data for an Equivalent Collision
Frequency of 12.82 Gc

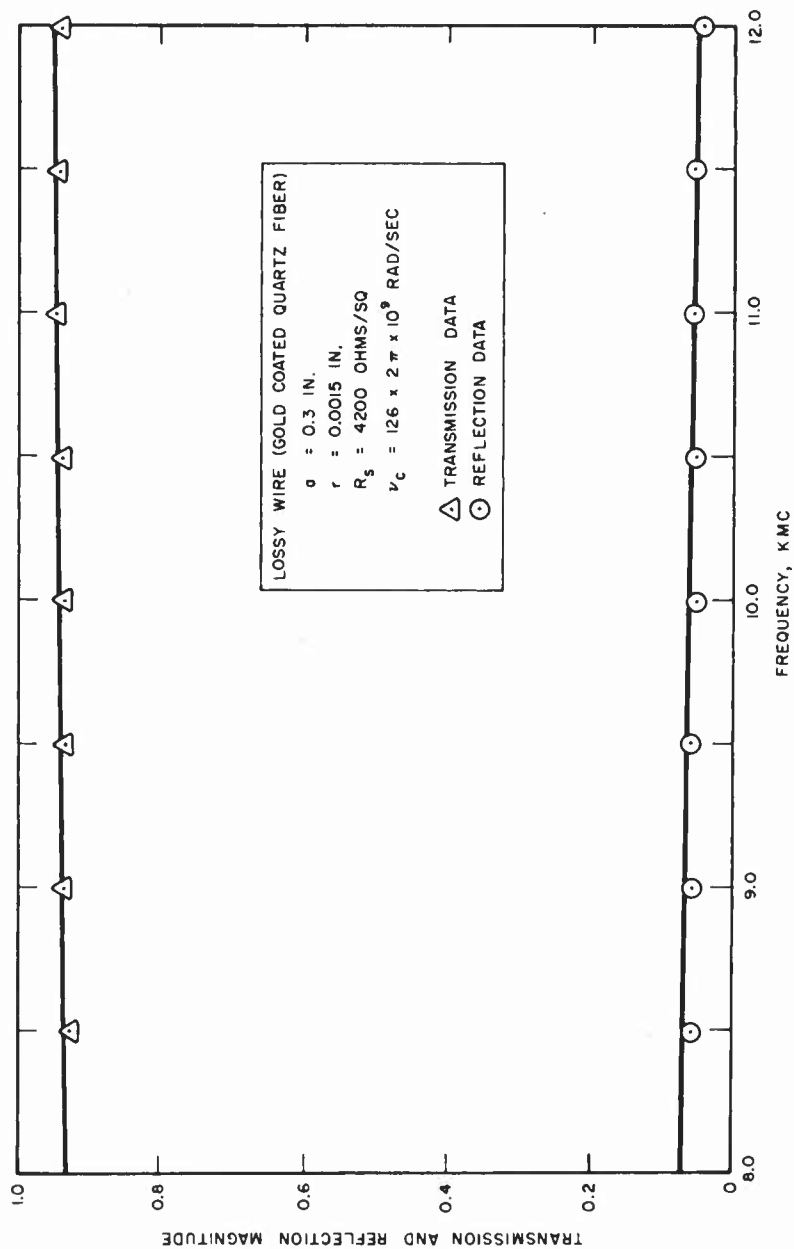


Fig. 15. Reflection and Transmission Data for an Equivalent Collision Frequency of 126 Gc

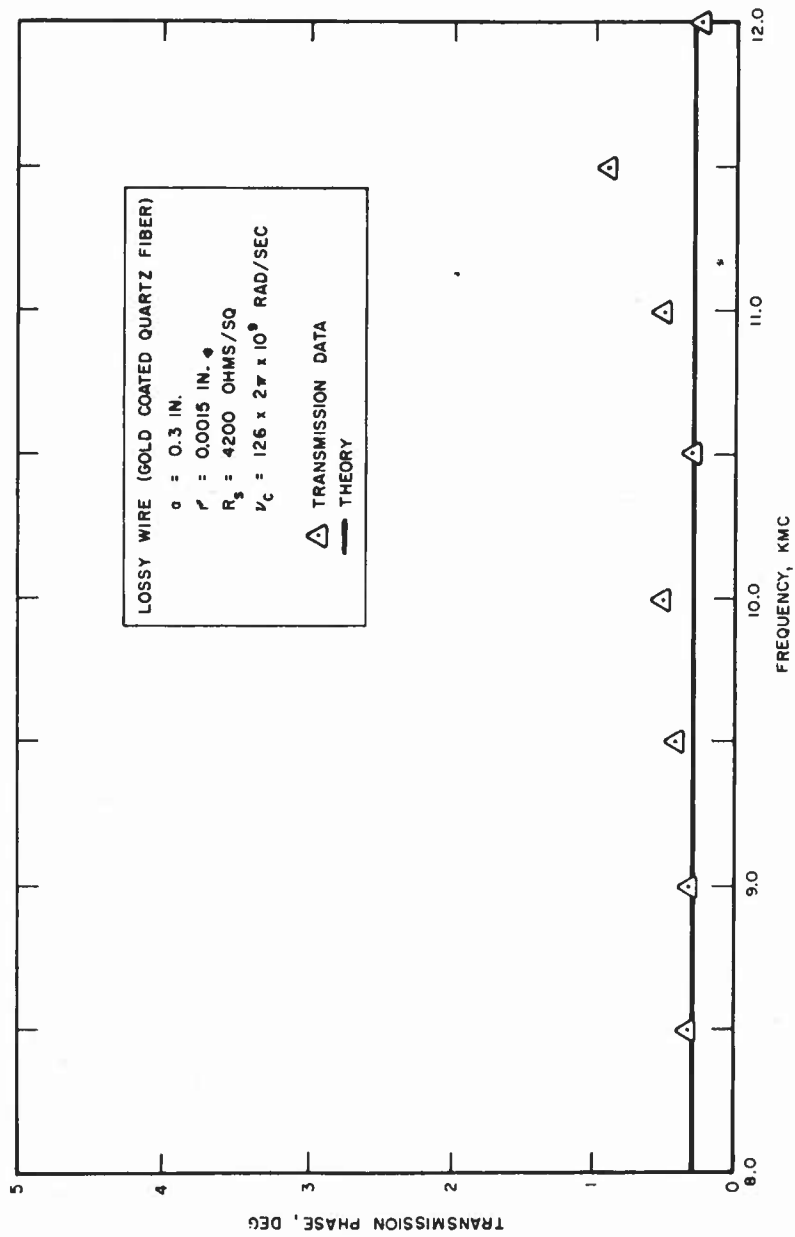


Fig. 16. Transmission Phase Data for an Equivalent Collision
Frequency of 126 Gc

surroundings. As the losses are increased, the surface impedance of the simulated sheath increases which, in turn, makes the reflections smaller.

Additional experimental data were obtained for a wire mesh structure. However, in this case, the wires making up the mesh were not orthogonal with the waveguide walls. The results indicate no measurable deviation in the reflection characteristics from the models having wires parallel to the electric field. The reflection and transmission coefficients, therefore, obey the relationships given by Eqs. (25) and (26) and are independent of the polarization of the incident fields.

VIII. SUMMARY

The simulation of a thin plasma sheath can be accomplished by using a square lattice screen structure when the following assumptions are valid

$$\frac{\omega_p}{\omega} \gg 1$$

$$k_o d \ll 1$$

Large collision frequencies can be simulated by using coated quartz fibers. Collision frequencies in the neighborhood of the operating frequency are realizable by this method. The experimental data confirm that the grid structure will simulate the impedance characteristics of a thin plasma sheath. The values of W^2D and V for the coated fiber grid structures are in a range which characterizes the sheaths developed around slender body re-entry vehicles. Plasma sheath simulation with a grid structure could therefore be useful in ground testing and evaluation of re-entry antenna systems.

REFERENCES

1. W. Rotman, "Plasma Simulation by Artificial Dielectric and Parallel-Plate Media," I. R. E. Trans. on Antennas and Propagation, Vol. AP10 No. 1, pp. 82-95, January 1962.
2. J. R. Wait, "The Electromagnetic Fields of a Dipole in the Presence of a Thin Plasma Sheet," Appl. Scientific Research, Vol. 8 Section B, pp. 397-417, 1960.
3. R. G. Jahn, "Interaction of Electromagnetic Waves and Slightly Ionized Gases," Calif. Inst. of Tech., Pasadena, Calif., AF49(638)-758, p. 15, August 1960.
4. E. C. Taylor, "Approximate Boundary Conditions for Plasma Sheaths," to be published as an Aerospace report, El Segundo, California.
5. J. K. Skwirzynski and J. C. Thackray, "Transmission of Electromagnetic Waves Through Wire Gratings (theory)," Marconi Review, Vol. 22, Second Quarter, pp. 77-90, 1959.
6. E. Goodall and J. Jackson, "Transmission of Electromagnetic Waves Through Wire Grating (experimental)," Marconi Review, Vol. 22, Second Quarter, pp. 91-98, 1959.
7. J. Brown, "Artificial Dielectrics Having Refractive Indices Less than Unity," Proc. I. E. E., Monograph No. 62R, Vol. 100, Part 4, pp. 51-62, May 1953.
8. G. G. MacFarlane, "Surface Impedance of an Infinite Parallel-wire Grid at Oblique Angles of Incidence," Journal I. E. E., (London), Part IIIA, Vol. 93, pp. 1523-1527, 1947.
9. E. A. Lewis and J. P. Casey, "Electromagnetic Reflection and Transmission by Gratings of Resistive Wires," Appl. Phys., Vol. 23, pp. 605-608, June 1952.
10. N. Marcuvitz, "Waveguide Handbook," (McGraw-Hill Book Co. Inc., New York, N. Y.), Vol. 10, p. 285, 1951.
11. P. Moon and D. E. Spencer, "Foundations of Electrodynamics," (Van Nostrand Co., Princeton, N. J.), p. 199, 1960.

DISTRIBUTION

Internal

Aseltine, J. A.
Barlow, E. J.
Batdorf, S. B.
Becker, R. A.
Billings, B. H.
Getting, I. A.
Hartunian, R. A.
Hlavka, G. E.
Logan, J. G.
Mager, A.
Mirels, H.
Moss, B.
Payne, R. E.
Pearce, K.
Targoff, W. P.
Weiss, M. T.
Betchov, R.
Bleviss, Z. O.
Caron, P. R.
Comisar, G. G.
Griesser, W. A.

Dazey, M. H.
Dix, D. M.
Eastmond, E. J.
Fuhs, A. E.
Golden, K. E.
Grewal, M. S.
Huddleston, R. H.
Kolpin, M. A.
Leonard, S. L.
Light, G. C.
Lu, A. Y.
McPherson, D. A.
Meyer, R. X.
Pridmore-Brown, D. C.
Stewart, G. E.
Taylor, E. C.
Turner, E. B.
Wood, J. G.
Phillips, R. C.
Smith, T. M.

External

Defense Documentation Center
Cameron Station
Alexandria, Virginia

SSD (SSTRE/Maj. Lewis, Jr.)

AFCRL (ERD Library)
L. G. Hanscom Field
Bedford, Mass.

AFCRL (CRRB)
L. G. Hanscom Field
Bedford, Mass.

AFOSR (Library)
Bldg. T-D
Washington 25, D. C.

HQ DDC
Bldg. 5
Cameron Station
Alexandria, Virginia

AFWL (Library)
Kirtland AFB
New Mexico

Library of Congress
Washington 25, D. C.

NASA (Library)
Ames Research Center
Moffett Fld, Calif.

HQ NASA
400 Maryland Ave., SW
Washington 25, D. C.

NASA (Library)
Langley AFB, Va.

AVCO
Wilmington, Massachusetts
ATTN: M. C. Adams

AVCO Everett Research Laboratory
2385 Revere Beach Parkway
Everett 49, Mass.
ATTN: A. Kantrowitz

AVCO Everett Research Laboratory
2385 Revere Beach Parkway
Everett, Mass.
ATTN: H. E. Petschek

Aeronutronic Division of Ford Motors
Corp.
Ford Road
Newport Beach, Calif.
ATTN: S. R. Byron

Bell Telephone Laboratory
Murray Hill, N. J.
ATTN: S. Buchsbaum

Boeing Scientific Research Laboratory
Seattle, Washington
ATTN: J. E. Drummond

Brooklyn Polytechnic Institute
Brooklyn 1, New York
ATTN: A. Ferri

Brooklyn Polytechnic Institute
Brooklyn 1, New York
ATTN: N. Markowitz

California Institute of Technology
1201 E. California
Pasadena, California
ATTN: J. D. Cole

NASA (Library)
Lewis Research Center
21000 Brookpark Road
Cleveland 35, Ohio

NASA (Library)
Marshall Space Flight Center
Huntsville, Alabama

National Bureau of Standards (Library)
Washington 25, D. C.

Naval Ordnance Lab. (Tech. Library)
White Oaks
Silver Springs 19, Maryland

Naval Research Lab.
Director, Tech. Info. Officer
Code 2000
Washington 25, D. C.

Oak Ridge National Lab (Library)
P. O. Box Y
Oak Ridge, Tennessee

Office of Tech Services
Tech. Reports Section
Dept. of Commerce
Washington 25, D. C.

ONR Branch
Commanding Officer
1030 Green Street East
Pasadena, Calif.

RADC (Library)
Griffis AFB, N. Y.

US Army Signal R & D Lab
(Data Equip. Br.)
Technical Info. Officer
Fort Monmouth, New Jersey

California Inst. of Technology
1201 E. California Street
Pasadena, California
ATTN: R. W. Gould

California Institute of Technology
1201 E. California Street
Pasadena, California
ATTN: L. Lees

California Institute of Technology
1201 E. California Street
Pasadena, California
ATTN: Library

California Institute of Technology
1201 E. California Street
Pasadena, California
ATTN: W. H. Liepmann

Convair - Astronautics Div.. of GDC
3165 Pacific Highway
San Diego, California
ATTN: H. Yoshihara

General Atomics
La Jolla, California
ATTN: R. H. Lovberg

General Atomics
La Jolla, California
ATTN: N. Rostoker

General Electric Co.
Knolls Research Laboratory
P. O. Box 1088
Schenectady, New York
ATTN: R. Alpher

US Atomic Energy Commission
(Dir of Research)
Washington 25, D. C.

US Atomic Energy Commission
Tech Info. Service Extension
P. O. Box 62
Oak Ridge, Tennessee

US Naval Research Lab. (Library)
Washington, D. C.

Wright Air Development Center
(Library)
Wright-Patterson AFB, Ohio

SSTP - Capt. D. De Bus

AF Avionics Laboratory
Wright-Patterson AF Base, Ohio
ATTN: R. Stimmel, AVW

General Electric Co.
Knolls Research Laboratory
P. O. Box 1088
Schenectady, New York
ATTN: H. Hurwitz

General Electric Co.
MAVD, Valley Forge
Philadelphia, Pennsylvania
ATTN: L. Steg

High Altitude Observatory
Boulder, Colorado
ATTN: S. Chapman

Hughes Research Laboratory
Malibu, Calif.
ATTN: R. C. Knechtli

I. I. T. Research Institute
10 W. 35th Street
Chicago, Illinois
ATTN: S. W. Kash

Johns Hopkins University
Department of Aeronautics
Baltimore 18, Maryland
ATTN: F. H. Clauser

Lockheed Missile and Space Center Sunnyvale, California ATTN: R. Landshoff	New York University Institute of Mathematical Sciences 25 Waverly Place New York 3, New York ATTN: H. Grad
Los Alamos Scientific Laboratory P. O. Box 1663 Los Alamos, New Mexico ATTN: J. M. B. Kellog	Northwestern University Department of Physics Evanston, Illinois ATTN: R. Hines
Los Alamos Scientific Laboratory Los Alamos, New Mexico ATTN: C. L. Longmire	Northwestern University Evanston, Illinois ATTN: A. B. Cambel
Massachusetts Institute of Technology Cambridge 39, Mass. ATTN: E. E. Covert	Princeton University Physics Department Princeton, New Jersey ATTN: E. A. Frieman
Massachusetts Institute of Technology Cambridge 39, Mass. ATTN: D. J. Rose	Princeton University Physics Department Princeton, New Jersey ATTN: T. H. Stix
Massachusetts Institute of Technology Dept. of Mechanical Engineering Cambridge 39, Mass. ATTN: J. L. Kerrebrock	Princeton University Project Matterhorn Princeton, New Jersey ATTN: M. B. Gottlieb
Massachusetts Institute of Technology Research Laboratory of Electronics Cambridge 39, Mass. ATTN: S. C. Brown	Rand Corporation 1700 Main Street Santa Monica, California ATTN: C. Gazley, Jr.
NASA Ames Research Center Moffett Field, Calif. ATTN: V. J. Rossow	Space Technology Laboratories, Inc. 1 Space Park Redondo Beach, Calif. ATTN: S. Alshuler
NASA Langley Field Research Center Langley, Virginia ATTN: A. Busemann	Space Technology Laboratories, Inc. 1 Space Park Redondo Beach, California ATTN: D. Langmuir
NASA Lewis Research Center 21000 Brookpark Road Cleveland 35, Ohio ATTN: W. Moeckel	Stanford University Stanford, California ATTN: D. Bershader
NASA Marshall Space Flight Center Huntsville, Alabama ATTN: E. Stuhlinger	

Stanford University
Stanford, California
ATTN: O. Buneman

Stevens Institute of Technology
Department of Physics
Hoboken, New Jersey
ATTN: George Schmit

Stanford University
Stanford, California
ATTN: P. Sturrock

University of California
Berkeley, California
ATTN: A. Trivelpiece

University of California
Physics Department
Berkeley, California
ATTN: A. Kaufmann

University of California
Physics Department
Berkeley, California
ATTN: W. B. Kunkel

University of California
Lawrence Radiation Laboratory
Berkeley, California
ATTN: J. M. Wilcox

University of California
Lawrence Radiation Laboratory
P. O. Box 808
Livermore, California
ATTN: W. Heckrotte

University of California
Lawrence Radiation Laboratory
P. O. Box 808
Livermore, California
ATTN: C. Van Atta

University of California
Physics Department
Los Angeles 24, Calif.
ATTN: A. Banos, Jr.

University of California
Physics Department
Los Angeles, Calif.
ATTN: B. D. Fried

University of California
School of Engineering
Los Angeles 24, Calif.
ATTN: N. Rott

University of Chicago
Enrico Fermi Institute for
Nuclear Studies
Chicago 37, Illinois
ATTN: S. K. Allison

University of Colorado
Physics Dept.
Boulder, Colorado
ATTN: W. E. Brittin

University of Illinois
Department of Electrical Engineering
Urbana, Illinois
ATTN: Paul D. Coleman

University of Illinois
Physics Department
Urbana, Illinois
ATTN: D. Jackson

University of Maryland
College Park, Maryland
ATTN: J. M. Burgers

University of Maryland
College Park, Maryland
ATTN: S. I. Pai

University of Michigan
Ann Arbor, Michigan
ATTN: O. Laporte

University of Minnesota
Physics Department
Minneapolis, Minnesota
ATTN: P. Kellog

University of North Carolina
Physics Department
Chapel Hill, North Carolina
ATTN: W. H. Bennett

University of Southern California
Los Angeles 7, California
ATTN: A. Kaprelian

University of Tennessee
Dept. of Physics and Astronomy
Knoxville, Tennessee
ATTN: E. G. Harris

US Naval Research Laboratory
Washington, D. C.
ATTN: A. C. Kolb

Westinghouse Research Laboratories
Beulah Road
Pittsburgh 35, Penna.
ATTN: R. E. Fox

Electro Optical Systems, Inc.
125 No. Vinedo
Pasadena, California
ATTN: A. T. Forrester

General Electric Co.
Valley Forge Space Technology Center
P. O. Box 8555
Philadelphia 1, Penna.
ATTN: S. M. Scala

Richard G. Fowler
Dept. of Physics
University of Oklahoma
Norman, Oklahoma

Henry August
North American Aviation
Los Angeles Division
D/282-130
Los Angeles, California